International Forum on Aeroelasticity and Structural Dynamics
IFASD 2026
16-18 June 2026, Göttingen, Germany

HAP-ALPHA: MODEL UPDATING BASED ON GROUND VIBRATION TEST AND THE INFLUENCE ON LOADS AND AEROELASTICITY

Arne Voß[1], Ralf Buchbach[1], Keith Soal[1], Robin Volkmar[1], Carsten Thiem[1], Julian Sinske[1], Janto Gundlach[1], Steffen Niemann[2]

[1] DLR - German Aerospace Center
Institute of Aeroelasticity
Bunsenstr. 10, 37073 Göttingen, Germany
Corresponding author: arne.voss@dlr.de

[2] DLR - German Aerospace Center
Institute of Lightweight Systems
Lilienthalplatz 7, 38108 Braunschweig, Germany

Keywords: highly elastic aircraft, model updating, loads, aeroelasticity

Abstract: This work presents the results of a ground vibration test of the highly elastic HAP-alpha (High Altitude Platform) and the subsequent model updating. The preliminary FE model was found to be sufficient for a meaningful aeroelastic design and a reliable structural sizing of this highly elastic aircraft. The steps for the model updating procedure, based on the experimental modal analysis, are described in detail. The agreement between the experimental and the updated FE modes is very good and all relevant modes are included. Good correlation was achieved for a frequency range of up to 15.0 Hz, which is more than sufficient for the intended aeroelastic applications. The required changes to the stiffness distribution are moderate (significant but not excessive) and can be explained in most cases.

1 INTRODUCTION AND MOTIVATION

The HAP-alpha (High Altitude Platform) is a very light weight, high altitude and long endurance aircraft (HALE) designed to stay airborne and hold position for several days at an altitude between FL450 and FL800. Carrying optical and radar measurement equipment, this allows scientists to make observations of the earth continuously for a long period of time by holding position. This is an advantage compared to satellites, which typically pass the same spot only every couple of days and fly much higher, leading e.g. to a lower optical resolution. The ability to start and land allows to re-configure and re-locate the aircraft for new and different missions. In addition, purchase and operation costs of an aircraft are expected to be much lower compared to those of a satellite, including the required infrastructure (airfield vs. spaceport).

A 3D rendering image of the HAP-alpha configuration, currently under development at the DLR [31], is shown in Figure 1. The idea is to create an extremely light weight aircraft (m_{design} = 136 kg) that flies very slowly (V_{EAS} = 9.0 to 11.0 m/s) but is highly efficient in terms of propulsion and aerodynamic performance (AR = 20) and is powered by solar electric energy. A team of specialists from different flight-physical disciplines designed this aircraft [19–21,42–44] on the edge of the physically possible. Because many design aspects are driven by aeroelasticity [38–40], the validation of the aeroelastic modeling is essential and the aircraft has a comprehensive flight test instrumentation (FTI) dedicated to the measurement of loads and the elastic response of the aircraft [41].

This paper presents the results of the ground vibration test (GVT) in comparison with the structural modeling using finite elements (FE). The steps for the model updating procedure are described in detail. With the updated models, the influence of the GVT on loads and aeroelasticity is analyzed, leading to a flight clearance. How good/reliable was the FE model used for the aeroelastic design? That is a key questions which are addressed in this work.

2 LITERATURE REVIEW

Although a few comparable aircraft are under development by various companies, scientific publications are rare and most of the following sources are press statements, newspaper articles, etc. This is in contrast to DLR’s own development HAP-alpha, where significant literature is published by the researchers working on the project (see above). A good general overview of high-altitude platform systems and their possible applications is given by Grest [46] or Fladeland [10]. Aircraft that already achieved their first flight include the EAV-4 [26,27] by the Korean Aerospace Research Institute and the Swift SULE [49], both with a surprisingly similar design. Scaled demonstrators were flown by Kea Aerospace [45,47] and India’s National Aerospace Laboratories (NAL) [48]. BAE selected a slightly different design for their PHASA-35 [24] and also passed their first flight successfully. Structural dynamic aspects of the Airbus Zephyr are presented by Benassi and Aquilini [2], however this was predominantly an overview paper. An accident report on Zephyr’s in-flight break-up [1] shows the challenges of operating such an aircraft. Many large companies such as Google [12] and Facebook [3,5,6] showed initial interest, but quickly stopped their projects. NASA’s prototype Helios [32] and the Solar Impuls [34] are differ in concept and mission. To the

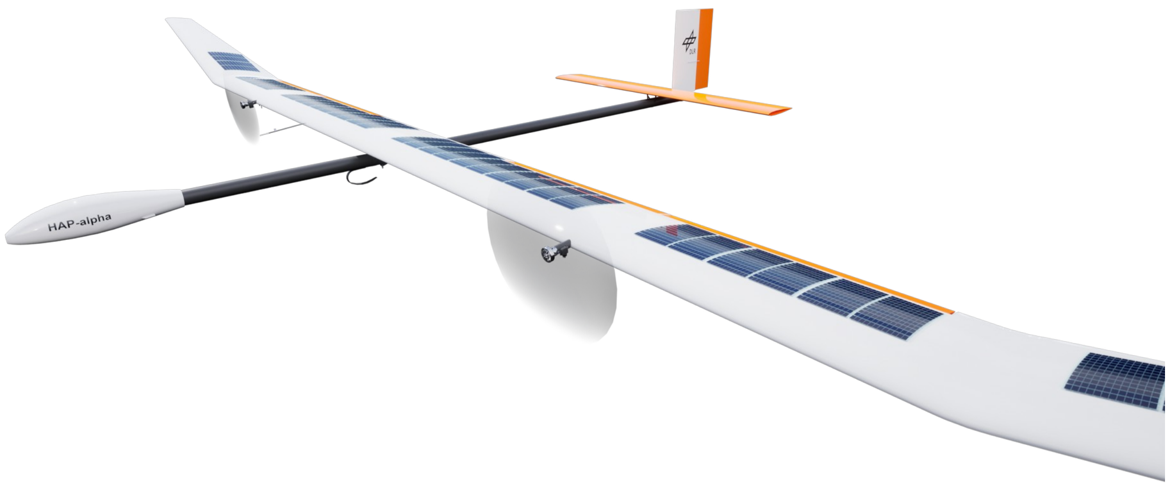

Figure 1: 3D rendering of the HAP-alpha (High Altitude Platform).

authors’ best knowledge, there are no publications with respect to model updating and ground vibration testing of such a vehicle from any of the mentioned companies.

While this publication focuses mainly on the application of model updating, a good overview of the theoretical background is provided by Mottershead and Friswell [11,30] or Link [28,29]. Research concerning uncertainty quantification and the influence of joints is presented by Govers and Link [17,18]. Although every aircraft manufacturer is required to perform a GVT for certification of a new aircraft model, their results are rarely published, not to mention the correlation with the numerical model. One of the few exceptions is Göge [13], who presented the model updating of a large transport aircraft with four engines (presumably A340, unconfirmed). For the updating, the first 28 elastic modes were considered, which include 13 engine modes. A recent publication by Holmberg [23] shows the model updating of Saab’s Gripen E. Due to the compact, non-slender shape of a military aircraft, only a few elastic modes of the airframe itself were considered. Instead, the stiffness of the attachment point was very important as well as the influence of multiple mass configurations. More literature is available from academic applications such as wind tunnel models or scaled demonstrators [7,9,14,16,33]. Their difference (compared to HAP-alpha) is mainly the complexity of the configuration – the more components the aircraft has, the more modes need to be considered and the more difficult the model updating becomes. To the authors’ best knowledge, there is no publication that evaluates the influence of GVT results on other aeroelastic disciplines and/or the necessary changes to the design or limitations imposed on the operational envelope.

3 STRUCTURAL AND MASS MODELING

Because of the slender, beam-like structure of the configuration, mainly beam and bar elements are used to model the structure, see Figure 2 a). The element stiffness and material characteristics are provided by the DLR Institute of Lightweight Systems and are converted to a finite element model for MSC.Nastran using a combination of the parameterized model generator ModGen [25] and spreadsheets.

All masses are modeled as concentrated masses (CONM2) and attached to the closest structural grid points. The masses comprise structural and system masses, visualized in Figure 2 b) and c) respectively.

The elastic mode shapes, visualized in Figure 3, are calculated from the updated model for the aircraft in the GVT configuration. It can be seen that the range of frequencies is low compared to typical large transport aircraft, starting with the 2n wing bending at 1.00 Hz. The 2n wing inplane mode at 1.38 Hz is also very low in frequency and closely spaced to the 2n wing bending. The relative motion of components, such as wing-fuselage or HTP-fuselage, are also found at very low frequencies due to the light-weight and consequently soft connecting structure. This results in a very high modal density in the frequency range under 10 Hz.

a) Stiffness model

b) Structural masses

c) System masses

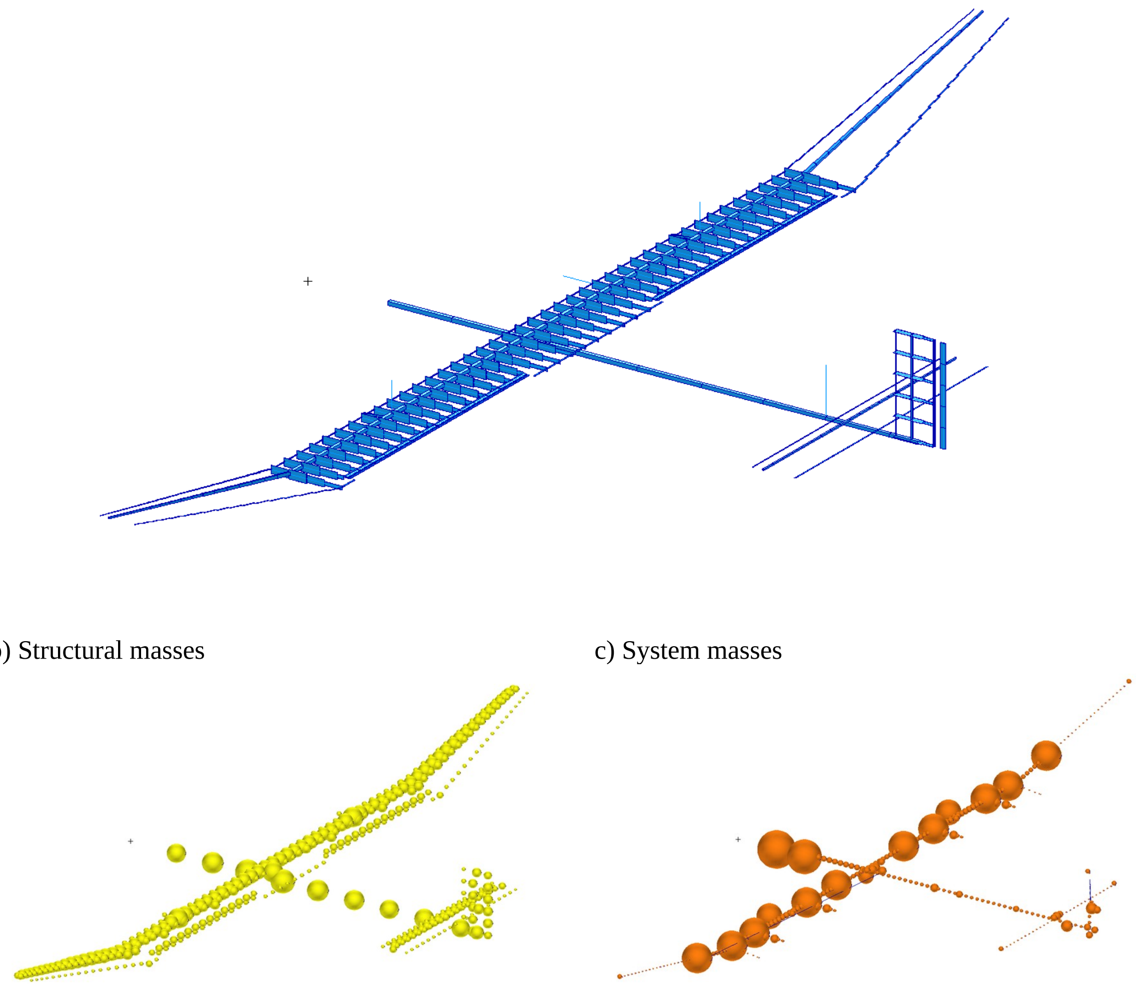

Figure 2: FE modeling of the HAP-alpha (High Altitude Platform).

Mode 1: 2n wing bending, 1.0 Hz

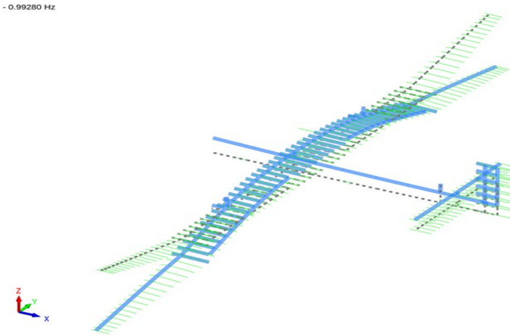

Mode 2: 1n wing inplane, scissor mode, 1.4 Hz

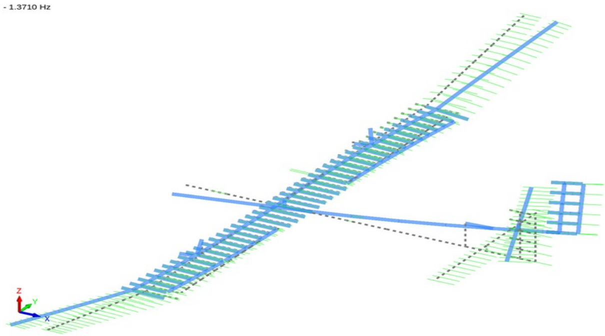

Mode 3: 2n wing inplane, 1.5 Hz

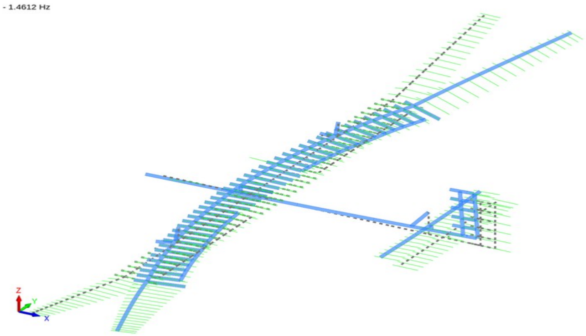

Mode 4: 3n wing bending, with HTP roll, 2.4 Hz

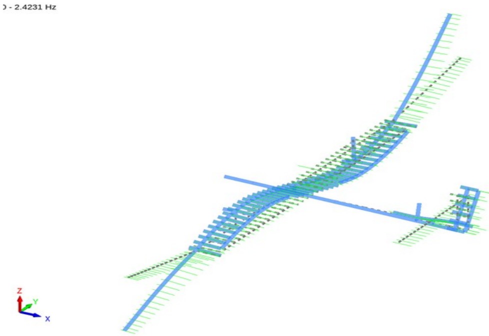

Mode 5: 3n wing inplane, with HTP yaw, 3.3 Hz

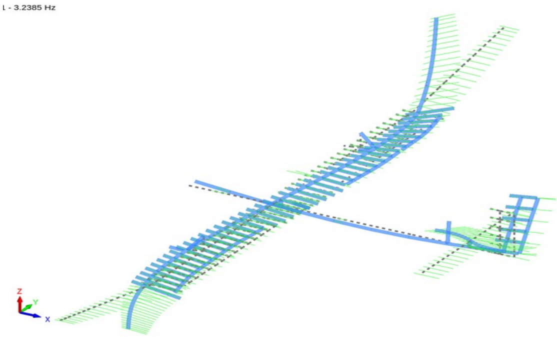

Mode 6: 1n HTP inplane, 3.6 Hz

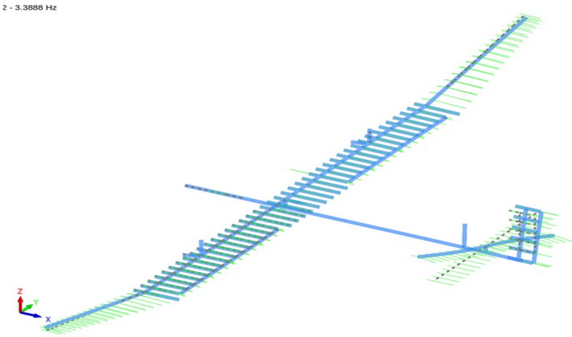

Mode 7: HTP roll / Tail rock, 3.4 Hz

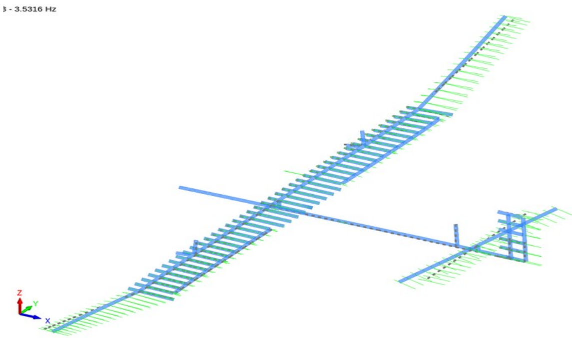

Mode 8: 4n wing bending with fuse. bending, 3.8 Hz

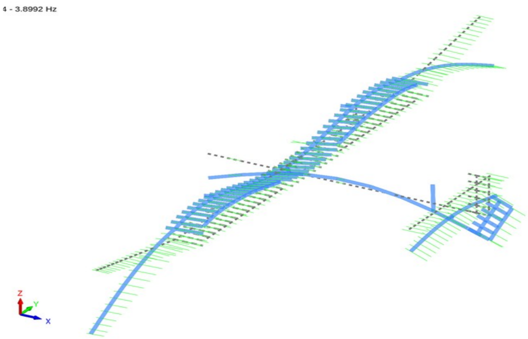

Figure 3: First eight elastic mode shapes of the updated FE model.

4 OVERVIEW OF GROUND VIBRATION TEST

The Ground Vibration Test (GVT) was performed efficiently by specialists of the DLR Institute of Aeroelasticity and marks a significant milestone on the path towards flight testing. Figure 4 shows the aircraft in a hangar at DLR's National Experimental Test Center for Unmanned Aircraft Systems located in Cochstedt, Germany. In general, this GVT was performed with the same methodologies, the same measurement hardware and the same quality controlled processes as for every large-scale GVT of commercial transport aircraft [15,35]. Because more details are given in a companion publication [36], this sections focuses on the topics relevant for the subsequent model updating.

The test was performed on the complete aircraft structure with only very few missing parts (the landing skids and some aerodynamic fairings were still to be manufactured). Those add-on parts have no influence on the primary aircraft structure and their mass was accounted for by dummy masses in the respective locations. Although not yet fully functional, all aircraft systems were present in terms of mass, too. Because there is no fuel, no passengers and no cargo, the aircraft has only two mass configurations that differ in the size of the solar generators. All structural components and systems were weighted, leading to a very close match with the total mass (residual < 200 g) as well as center of gravity (residual < 1.0 mm).

As can be seen in Figure 4, the aircraft was tested without the upper and lower foil-type skin. This decision allows to access the primary structure to mount both sensors and shakers and it reduces the influence of the surrounding, co-moving air significantly, which is important considering that the aircraft is very light-weight and the mass ration of air/structure would be

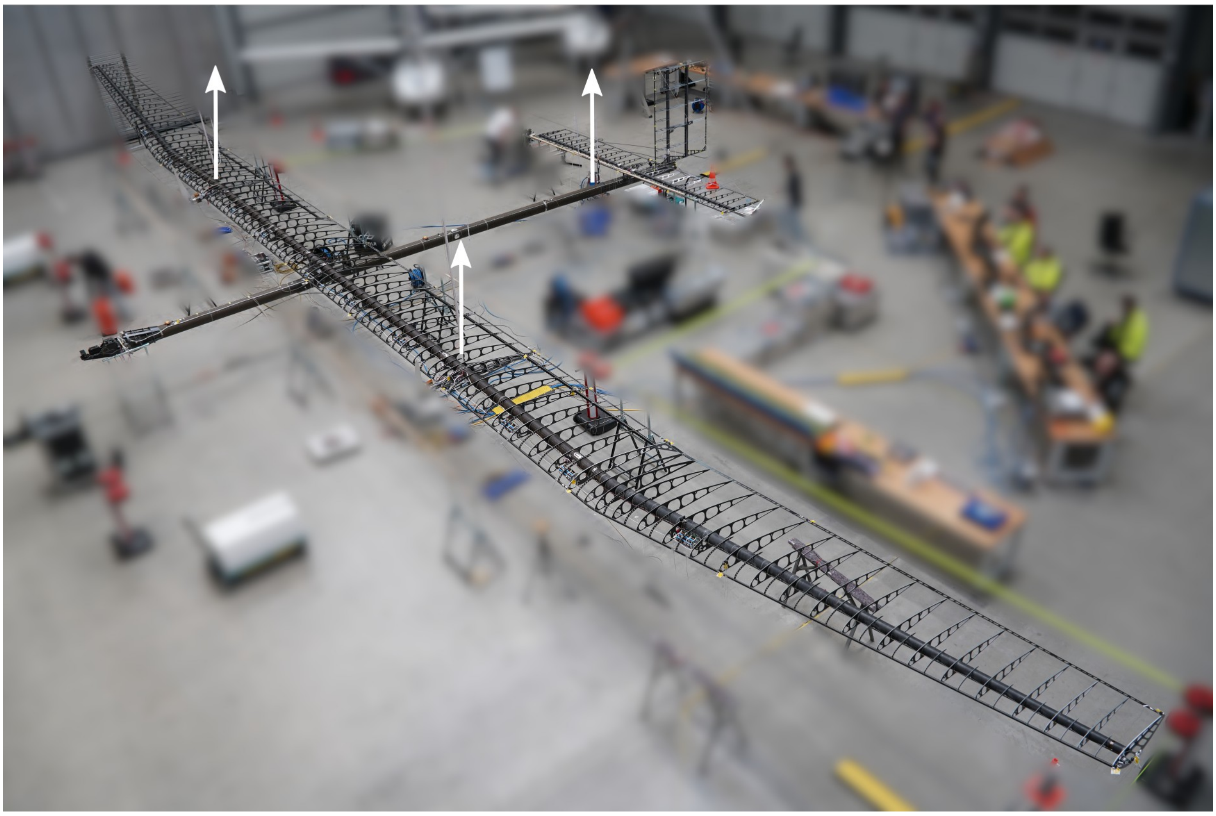

Figure 4: The HAP-alpha (High Altitude Platform) during the ground vibration test, bungee suspension indicated in white.

very low. The mass (≈3.5 kg) and stiffness of the skin was removed from the FE model and a study showed that the two effects cancel out nicely for many modes, leading to negligible changes in frequency.

For the boundary condition, a three-point bungee suspension was selected. The bungee locations (left / right engine pylon and tail, indicated in Figure 4 by white arrows) were chosen in such a way that the elastic deformations of the aircraft remain small and to avoid excessive roll or yawing motion of the aircraft during the test. The bungee selection was driven by the rigid body heave motion, whose frequency was desired to be as low as possible to allow a good separation from the first wing bending frequency, predicted at 0.95 Hz. The selection was a compromise between bungee length, stiffness, strength and availability. For example, the length decreases the overall stiffness, but the available height of the building is limited. Although a low bungee stiffness is desired, an excessive total deflection is unpractical from a handling point of view. Next, the bungee strength must be sufficient to carry the aircraft and finally, the bungees should be in their linear elastic range under loading. The bungees were redirected by pulleys (26” bicycle wheels) mounted to the hangar roof, and attached to counter masses on the ground, leading to a nominal length of 14.5 m at the pylons and 16.4 m at the tail. At each pylon, a bundle of three latex bungees with 14.0 mm diameter was used while at the tail, three 4.5 mm bungees were sufficient. The bungees were added to the FE model, leading to a predicted heave motion of 0.19 Hz. In addition, a study showed that the selected set-up yields elastic modes very close to the free-free condition.

A total number of 117 acceleration sensors at 85 measurement positions, specified in more detail in [36], was installed on the aircraft, together with shaker attachment hardware at 8 excitation locations. The total additional mass accumulated to 3.0 kg and was added to the FE model. Also, for each sensor a corresponding FE node was identified (or added where necessary) such that each sensor has a numerical partner.

The FE model, presented in Section 3, was adapted to the GVT configuration already before the test and imported into the DLR Correlation Tool [4] to allow for a first on-site correlation between test and numerical results.

5 MODEL UPDATING

In an initial step, all structural and system masses are manually updated in the FE model, leading to high level of trust because of the detailed modeling and cross-check with the total aircraft mass and the center of gravity. Consequently, only the stiffness is adjusted in the following. Because the geometry of the primary structure is known, the author also has trust in the second area moments $I_{1,2}$ and the torsional constant J of the beam elements, leaving the material properties E and G as variables. The variables are applied per segment, for example with eight segments along the wing and four segments for the fuselage, corresponding to the way the tubes are manufactured. A physical interpretation of the variables could be the variation in the actual material properties, but changes also account for imperfections, idealizations and simplifications made in the modeling, as Holmberg [23] points out.

Due to the time frame of the model updating, only existing methods were applied, implemented in the FEMtools [8] software. The model updating is performed as a least squares optimization with the delta frequency (ΔF) and/or the modal assurance criterion

(MAC) value between finite elements modes (FE) and experimental modal analysis (EMA) as residue. The general strategy was to split the model updating into multiple steps, listed in Table 1, working only with a small group of modes and variables at the same time. In some cases, a number of secondary modes were added to the optimization to make sure that while improving the targeted mode, the secondary modes don’t deteriorate. A sensitivity analyses prior to the optimization helped to confirm the right parameters are selected for the modes in question. In some cases, manual adjustments are necessary because of the limitations of the optimization algorithms. For example, the optimization always needs a mode shape pair and, in some cases, looses track of the pairs. Another shortcoming of the automated optimization is the inability of the algorithm to move a structural dynamic feature (e.g. HTP roll) over a large frequency range or across multiple modes.

Step	Modes	FE Parameters
1	Heave Roll	Bungee stiffness
2	2n wing bending 3n wing bending 4n wing bending	Young's modulus of wing segments
3	2n wing inplane	Young's modulus of leading and trailing edges
4	fuselage bending lateral fuselage bending vertical	Young's modulus of fuselage segments
5a	2n HTP bending VTP bending	Young's modulus of HTP and VTP main spars
5b	2n HTP inplane VTP inplane	Young's modulus of leading and trailing edges
6	1n wing inplane 3n wing bending, with HTP roll 3n wing inplane, with HTP yaw 1n HTP inplane HTP roll / Tail rock	Torsional spring stiffness (roll and yaw) at wing/HTP-fuselage connection
7	sym wing torsion asym wing torsion, with VTP asym wing torsion, pure 2n wing bending 2n wing inplane 3n wing bending 5n wing bending fuselage bending vertical	Young's and shear modulus of wing segments Young's modulus of fuselage segments
8	VTP bending VTP bending, with rudder asym wing torsion, with VTP VTP inplane	Young's and shear modulus of VTP main spar Torsional spring stiffness of rudder attachment
9	3n wing bending, with HTP roll 3n wing inplane, with HTP yaw 1n HTP inplane HTP roll / Tail rock	Torsional spring stiffness (roll and yaw) at wing/HTP-fuselage connection
10	VTP inplane sym wing torsion	Young's modulus of VTP leading and trailing edges
11	4n wing inplane	Young's modulus of leading and trailing edges Iz of main spar

12	Smoothing step with all modes to find/confirm an overall optimum and catch cross-correlations	Young's and shear modulus of wing segments
13	3n wing bending, with HTP roll 3n wing inplane, with HTP yaw, in-phase 1n HTP inplane, with wing inplane, out-of-phase HTP roll / Tail rock fuselage bending lateral HTP pitch	Torsional spring stiffness (roll, yaw and pitch) of HTP-fuselage connection
14	VTP bending VTP bending, with rudder	Torsional spring stiffness of rudder attachment
15	Restoration step with all modes due to mass update of ailerons (influence on torsional mode shapes)	Young's and shear modulus of wing segments

Table 1: Model updating steps.

5.1 Results

The results from the experimental modal analysis (EMA) are compared to the finite elements modes (FE) in Table 2. Based on experience, a difference in frequency $\Delta F < 5\%$ and $MAC > 80\%$ is considered as a very good agreement by the author, indicated by green color in the table, while yellow represents values that are still acceptable. Generally speaking, the agreement between EMA and the updated FE modes is very good and all relevant modes are included. Also, the frequency range of up to 15.0 Hz is more than sufficient for the intended aeroelastic applications.

Mode	EMA [Hz]	FE before [Hz]	FE updated [Hz]	ΔF [%]	MAC [%]	Mode name, description
1	0.23	0.23	0.21	-7.1	75.2	a/c roll
2	0.25	0.25	0.24	-0.2	95.0	a/c heave
3	0.99	0.95	1.00	0.7	98.4	2n wing bending
4	1.39	–	1.38	-0.4	99.3	1n wing inplane, scissor mode, with HTP yaw
5	1.54	–	1.51	-1.7	94.7	2n wing inplane
6	2.48	2.33	2.44	-1.7	82.4	3n wing bending, with HTP roll
7	3.16	–	3.27	3.5	89.9	3n wing inplane, with HTP yaw, in-phase
8	3.46	–	3.56	2.9	86.9	1n HTP inplane, with wing inplane, out-of-phase
9	3.52	3.14	3.39	-3.8	95.1	HTP roll / Tail rock
10	3.63	3.35	3.84	5.6	98.8	4n wing bending, vertical fuselage bending, in-phase
11	4.74	–	4.93	4.2	81.6	4n wing inplane
12	4.79	–	4.93	2.9	73.5	fuselage bending lateral
13	5.44	4.83	5.32	-2.1	94.1	fuselage bending vertical
14	7.07	5.79	6.71	-5.1	96.8	5n wing bending
15	7.54	7.09	7.47	-0.9	98.7	2n HTP bending
16	7.75	7.34	7.75	0.0	85.4	VTP bending

17	8.14	–	-	-	-	5n wing inplane
18	8.17	6.60	8.87	8.6	81.0	asym wing torsion, with VTP bending in-phase
19	8.55	6.93	8.45	-1.2	81.2	sym wing torsion
20	8.91	–	8.94	0.4	82.7	2n HTP inplane
21	9.62	–	-	-	-	6n wing inplane
22	10.65	11.65	10.68	0.3	87.4	asym wing torsion, pure
23	10.85	–	10.75	-0.9	73.9	VTP inplane, with wing in-phase
24	11.39	11.99	11.89	4.4	73.4	6n wing bending
25	12.62	10.68	12.67	0.4	86.0	7n wing bending
26	13.32	–	-	-	-	7n wing inplane
27	14.56	–	14.58	0.1	90.4	HTP pitch
28	14.95	16.41	15.18	1.6	87.0	VTP bending, with rudder
29	15.04	–	16.90	12.4	66.3	8n wing bending

Table 2: Results from experimental modal analysis (EMA) compared to finite elements modes (FE).

Figure 5 shows the MAC matrix between EMA and FE modes, before and after model updating while the frequencies are listed in Table 2. A mixed agreement can be seen for the initial FE model, however, fundamental characteristics such as the 2n wing bending (before 0.95 Hz, updated 1.00 Hz) or the symmetrical wing torsion (before 6.93 Hz, updated 8.45 Hz) showed already an acceptable agreement in terms of frequency and shape. After the model updating, the MAC matrix shows a much clearer correlation along the diagonal and the number of correlated modes increased significantly. Note that some modes are very close in terms of frequency and may appear in switched order in the FE model.

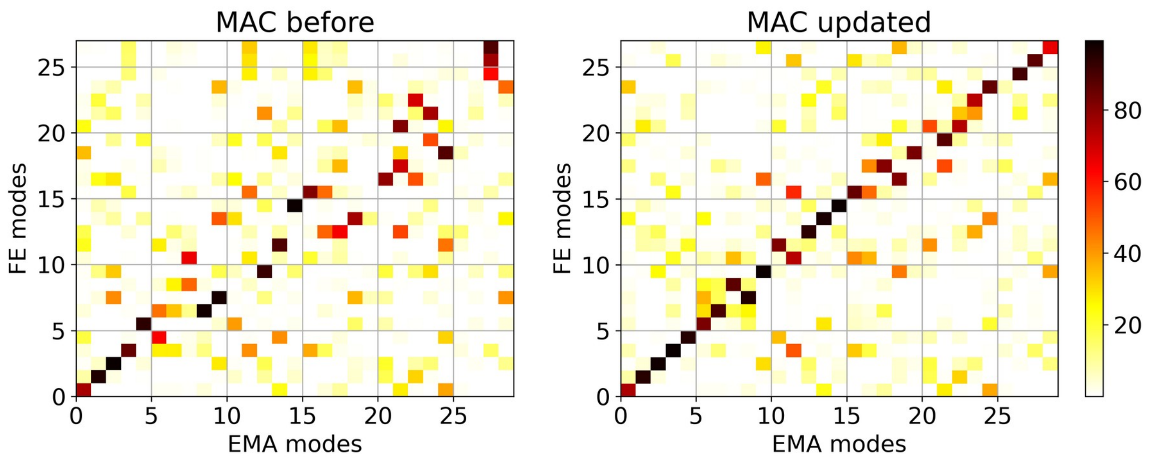

Figure 5: MAC matrix between EMA and FE modes, before and after model updating.

One interesting phenomenon are the inplane modes, which are typically of high(er) frequency and little interest/importance for an aeroelastic analysis. For the HAP-alpha, the inplane modes are of comparably low frequency due to the long, slender wings. In addition, there is a pronounced coupling between torsional and inplane motion of the wings due to the V-shaped outer wings (12°) and the corresponding out-of-plane masses. While 2n, 3n and 4n wing inplane could be assigned clearly in both models, the higher inplane modes are more difficult. For example, the 5n wing inplane (EMA mode 17) doesn't appear as an individual mode in the FE model, but can be found in the neighboring FE modes 16 and 18. The same is true for 6n wing inplane (EMA mode 21) while for 7n wing inplane (EMA mode 26), no partner is found in the FE model at all. Part of the explanation is that the required spatial resolution of sensors for a meaningful comparison is reached / exceeded, which is also one reason for a rapid decrease in correlation of all modes beyond 15.0 Hz.

The resulting stiffness distributions are shown in Figures 6 and 7. While the initial model is shown on the left hand side, the updated model is shown on the right hand side. Luckily, the required changes are moderate (significant but not excessive) and can be explained in most cases by the model shortcomings identified in the following Section 5.2.

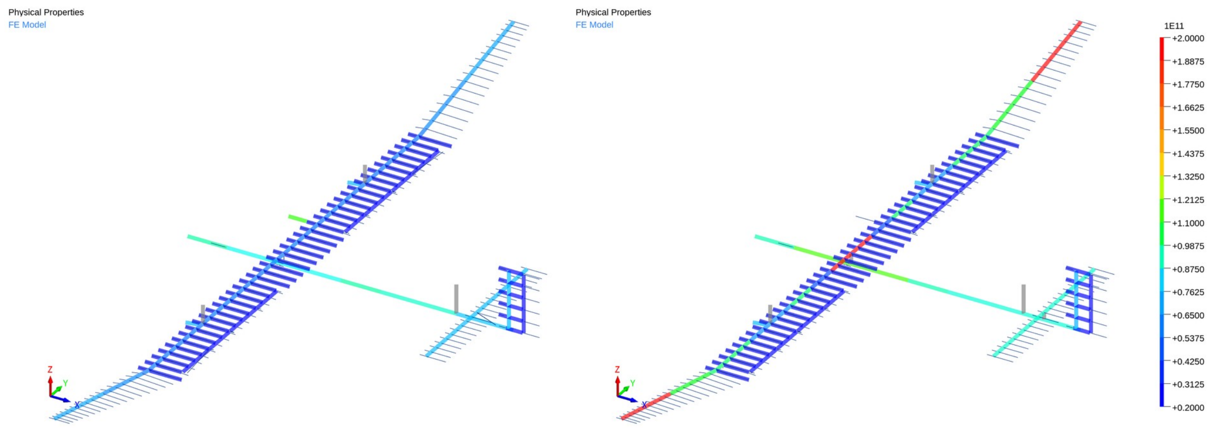

Figure 6: Young’s modulus, before and after model updating

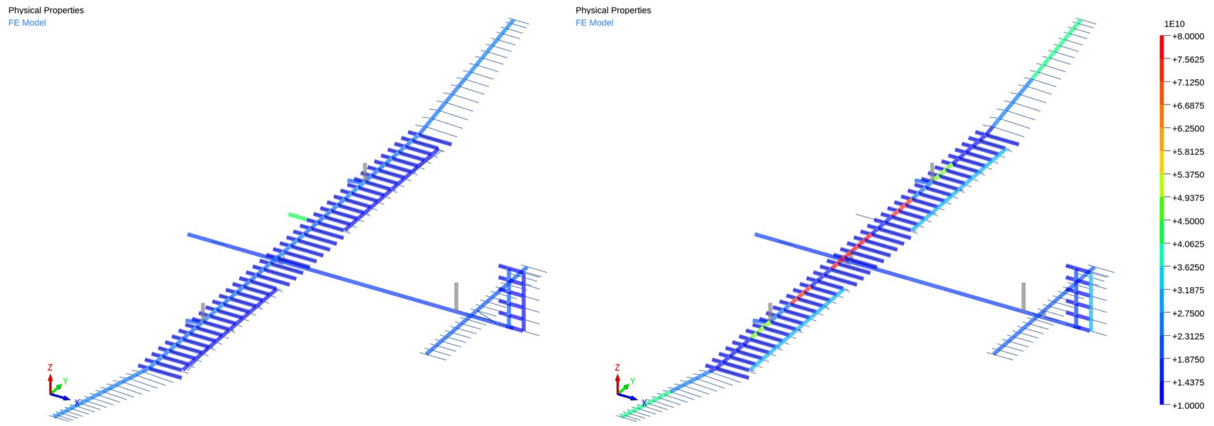

Figure 7: Shear modulus, before and after model updating.

Moving from the GVT configuration towards flight test, the following changes are applied:

- Remove bungee suspension
- Remove masses of GVT instrumentation
- Add skin to the FE model (mass + stiffness)

The MAC matrix, shown in Figure 8, reveals a close similarity between the two configurations. The biggest differences involve the HTP, as well as the wing torsion modes. For the HTP, one explanation is that the acceleration sensors are heavy compared to its structure and this changes the roll and yaw motion. The influence of the skin is largest for the torsional modes due to its second area moments about the torsional axis. Finally, the 4n wing inplane and the vertical fuselage bending modes mix. Still, the agreement is good and the differences with respect to the tested configuration are acceptable and explainable.

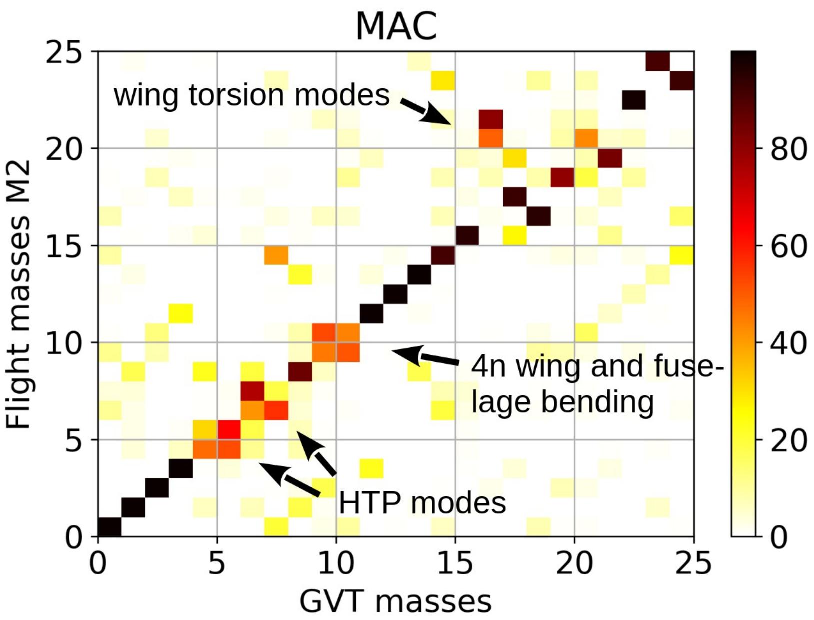

Figure 8: MAC matrix between GVT and flight configuration.

5.2 Model shortcomings

A known model shortcoming were the connections between the wing and the fuselage as well as between the HTP and the fuselage, where the stiffness was simply unknown, so that, in the absence of any better knowledge, the designated torsional spring connections were set to rigid. Especially the HTP can couple with nearly every other mode, depending on its roll and yaw stiffness, which turned out to be a challenge in the model updating and required repeated iterations (steps 6, 9 and 13). For future projects, an earlier estimation of the connection stiffness is recommended and would provide a better initial value for the model updating.

Another unexpected (but obvious) shortcoming were the leading and trailing edges (LE and TE), modeled as additional beam elements on the elastic axis and with an offset in chord direction (i.e. beam placed at the actual location but acting on the elastic axis). In reality, the connection of LE and TE to the main spar is via the ribs, made from thin (6 mm) composite sandwich material. In addition, the LE is discontinuous, so that the loads are not transferred equally via all ribs. Considering an inplane motion, the ribs are unable to transfer all forces to the LE and simply deflect in lateral direction. This leads to a significant over-estimation of the influence from LE and TE on the wing’s inplane stiffness and during the model updating, the young’s modulus of the LE and TE was decreased by one order of magnitude.

Local stiffening of the tube-type main spar led to a general under-estimation of its stiffness. For example, the inner and outer wing are joined (at the engine pylons) by an inner tube on a length of 800 mm, leading to a significant local reinforcement. Generally, the tubes are manufactured in eight segments, leading to an increased material thickness at the joints (approx. factor 1.5 on a length of 80-140 mm) plus an inner tube added for stability of the joint. Finally, at each rib, additional fibers are placed in radial direction on a length of “only” ~15 mm, but there are 38 ribs. Modeling these effects individually is not helpful/necessary, but they could be accounted for by a general, overall factor on the stiffness.

A global increase of stiffness was necessary at the outer wings, where the tube-type spar was much stiffer (and heavier) than expected after manufacturing – here the aircraft was simply not built to the specifications.

5.3 Improvements

For future ground vibration tests on similar aircraft and with the results presented above in mind, only a few things should be modified. For example, more sensors in x-direction would be useful (same resolution as for z-direction). In line with that, a dedicated excitation in x-direction might be helpful. From a practical point of view, a shorter suspension without a roller/pulley would be sufficient and lead to an easier handling.

Apart from that, having GVT specialists in-house was very useful for discussions and interpretation of results, for which the first author is very thankful. The DLR Correlation Tool [4] was not only useful on-site during the test, but also after the test to investigate mode families, to find missing modes and to gain a better understanding of the measurements.

6 LOADS AND AEROELASTIC ANALYSES

An extended version of the current paper, including a detailed analysis of the loads (envelope of e.g. the wing root bending and torsional moments Mx and My) and aeroelastic effects (e.g. control surface effectiveness, the flight shape and a flutter check), will be submitted to the CEAS Journal [37].

7 SUMMARY AND OUTLOOK

Due to the low eigenfrequencies and low overall mass, standard GVT procedures were adapted for the HAP-alpha aircraft. In this way, the structural and mass models could be updated efficiently. The steps for the model updating procedure are described in detail, leading to a good agreement with the experimental mode shapes and frequencies up to 15.0 Hz. With the updated model, the loads and aeroelastic analyses will repeated and compared to the pre-GVT results. The key take-aways from this work are:

- The preliminary FE model was sufficient to allow for a meaningful aeroelastic design and a reliable structural sizing of this highly elastic aircraft.
- The agreement between the experimental and the updated FE modes is very good and all relevant modes are included.
- Good correlation was achieved for a frequency range of up to 15.0 Hz, which is more than sufficient for the intended aeroelastic applications.

- The required changes to the stiffness distribution are moderate (significant but not excessive) and can be explained in most cases.

Currently, the calibration of the strain gages for load measurements (as part of the flight test instrumentation described in [41]) is under preparation. Once the flight readiness review is passed and the crew has sufficient training, the team is ready for flight test. The first flights in lower altitude [22] will take place in DLR's National Experimental Test Center for Unmanned Aircraft Systems located in Cochstedt, Germany, while flights in higher altitude are planned for Kiruna, Sweden or Tawhaki, New Zealand. Once the flight test of the aircraft itself is completed, two different measurement systems (an optical camera system and a synthetic aperture radar) will be installed as payload and tested in the lower stratosphere, followed by first scientific missions.

REFERENCES

[1] Australian Transport Safety Bureau, "In-flight break-up involving Airbus Zephyr unmanned aerial vehicle", Australian Transport Safety Bureau, Canberra, Australia, ATSB Transport Safety Report AO-2019-056, Sep. 2020.

[2] Benassi, L., and Aquilini, C., "The Structural Dynamics of Flying Non Stop for 100 Days", in *18th International Forum on Aeroelasticity and Structural Dynamics*, Savannah, Georgia, 2019.

[3] Bolandhemmat, H., "Flight Control System Design for a High Altitude, Long Endurance Airplane: Sensor Distribution and Flexible Modes Control". Facebook Research.

[4] Buchbach, R., Sinske, J., Govers, Y., and Böswald, M., "Database-supported correlation of modal data – the DLR Correlation Tool", in *Proceedings of ISMA 2024 - International Conference on Noise and Vibration Engineering and USD 2024 - International Conference on Uncertainty in Structural Dynamics*, Leuven, Belgien, 2024, https://elib.dlr.de/206457/.

[5] Colas, D., Roberts, N. H., and Suryakumar, V. S., "HALE Multidisciplinary Design Optimization Part I: Solar-Powered Single and Multiple-Boom Aircraft", presented at the AIAA Aviation, Atlanta, Georgia, 2018, https://doi.org/10.2514/6.2018-3028.

[6] Colas, D., Roberts, N. H., and Suryakumar, V. S., "HALE Multidisciplinary Design Optimization Part II: Solar-Powered Flying-Wing Aircraft", presented at the AIAA Aviation, Atlanta, Georgia, 2018, https://doi.org/10.2514/6.2018-3028.

[7] Di Leone, D., Lo Balbo, F., De Gaspari, A., and Ricci, S., "Model Updating and Aeroelastic Correlation of a Scaled Wind Tunnel Model for Active Flutter Suppression Test", *Aerospace*, vol. 8, no. 11, p. 334, Nov. 2021, https://doi.org/10.3390/aerospace8110334.

[8] Dynamic Design Solutions, "FEMtools". [Online]. Available at: https://www.femtools.com/. [Accessed: 04-Jul-2025].

[9] Ellmo, A., "Ground Vibration Testing and Model Updating of a Transconic Flutter Wind Tunnekl Model", presented at the International Forum on Aeroelasticity and Structural Dynamics, The Hague, The Netherlands, 2024.

[10] Fladeland, M., "High Altitude Platform Systems (HAPS) in support of NASA's Earth System Observatory - YouTube", presented at the Geoscience and Remote Sensing Society, Online, 10-Aug-2024, https://www.youtube.com/watch?v=Z3FKciUgLBM.

[11] Friswell, M., and Mottershead, J. E., *Finite element model updating in structural dynamics*, Reprinted. Dordrecht: Springer-Science + Business Media, B.V, 1996.

[12] Gibbs, S., "Google's Titan drones to take flight within months", *The Guardian*, 03-Mar-2015, https://www.theguardian.com/technology/2015/mar/03/googles-titan-drones-to-take-flight-within-months.

[13] Göge, D., “Automatic updating of large aircraft models using experimental data from ground vibration testing”, *Aerospace Science and Technology*, vol. 7, no. 1, pp. 33–45, Jan. 2003, https://doi.org/10.1016/S1270-9638(02)01184-7.

[14] Gonzalez, P., Guilherme, B., Quesada, Á., Stavorinus, G., Silvestre, F. J., Hilger, J., Hanke, C., Voß, A., and Krüger, W., “Wind tunnel testing and modal validation of TU-Flex’s high aspect-ratio wings”, presented at the International Forum on Aeroelasticity and Structural Dynamics, Den Haag, The Netherlands, 2024, https://elib.dlr.de/204977/.

[15] Govers, Y., Böswald, M., Lubrina, P., Giclais, S., Stéphan, C., and Botargues, N., “AIRBUS A350XWB Ground Vibration Testing: Efficient techniques for customer oriented on-site modal identification”, presented at the ISMA 2014, Leuven, Belgien, 2014, pp. 2503–2516, https://elib.dlr.de/91092/.

[16] Govers, Y., Jelicic, G., and Akbay, T., “The use of strain sensors for modal identification of aeroelastic structures”, in *27th International Conference on Noise and Vibration Engineering, ISMA 2016 and International Conference on Uncertainty in Structural Dynamics, USD2016*, Leuven, Belgien, 2016, pp. 2207–2216, https://elib.dlr.de/107712/.

[17] Govers, Y., and Link, M., “Model updating using uncertain experimental modal data”, in *Proceedings “IFASD 2011”*, Paris, Frankreich, 2011, https://elib.dlr.de/70272/.

[18] Govers, Y., and Link, M., “Stochastic model updating—Covariance matrix adjustment from uncertain experimental modal data”, *Mechanical Systems and Signal Processing*, vol. 24, no. 3, pp. 696–706, Apr. 2010, https://doi.org/10.1016/j.ymssp.2009.10.006.

[19] Hasan, Y., Fezans, N., and Voß, A., “Landing Simulation of a High-Altitude Platform with Skid-Type Landing Gear - Flight Procedure, Controller and Loads”, presented at the ICAS Congress, Stockholm, Sweden, 2022, https://elib.dlr.de/191048/.

[20] Hasan, Y. J., Fezans, N., and Voß, A., “Flight Mechanical Analysis of a Very Flexible High-Altitude Platform Under Uncertainty Considerations”, presented at the 34th Congress of the International Council of the Aeronautical Sciences, Florence, Italy, 2024.

[21] Hasan, Y. J., Roeser, M. S., Hepperle, M., Niemann, S., Voß, A., Handojo, V., and Weiser, C., “Flight mechanical analysis of a solar-powered high-altitude platform”, *CEAS Aeronaut J*, Nov. 2022, https://doi.org/10.1007/s13272-022-00621-2.

[22] Hasan, Y., Voß, A., Raab, C., and Fezans, N., “HAP-alpha: Developement of System Identification Manoeuvres for Low-Altitude Flight Testing of a Flexible High-Altitude Platform”, presented at the International Forum on Aeroelasticity and Structural Dynamics, Göttingen, Germany, 2026.

[23] Holmberg, E., “FE-Model update after GVT of a Gripen E test aircraft”, in *International Forum on Aeroelasticity and Structural Dynamics*, 2019, pp. 1–15, https://www.researchgate.net/profile/Erik-Holmberg-2/publication/334030255_FE-model_update_after_GVT_of_a_Gripen_E_test_aircraft/links/5d1327aea6fdcc2462a65311/FE-model-update-after-GVT-of-a-Gripen-E-test-aircraft.pdf.

[24] Kay, A., “PHASA-35 First Flight | Ground-breaking solar powered unmanned aircraft makes first flight”, *BAE Systems | International*, 17-Feb-2020. [Online]. Available at: https://www.baesystems.com/en/article/ground-breaking-solar-powered-unmanned-aircraft-makes-first-flight. [Accessed: 20-Feb-2020].

[25] Klimmek, T., “Parameterization of topology and geometry for the multidisciplinary optimization of wing structures”, in *CEAS 2009 - European Air and Space Conference*, Manchester, United Kingdom, 2009.

[26] Korea Aerospace Research Institute, “KASA Successfully Conducts Low-Altitude Flight Test of Stratospheric Drone”. [Online]. Available at: https://www.kasa.go.kr/bbs/BBSMSTR_000000000041/B000000001828Wu2sA1.do?mno=sub01_01. [Accessed: 18-May-2026].

[27] Korea Aerospace Research Institute, “Stratospheric Solar-Powered Electric UAVs”.

[Online]. Available at: https://www.kari.re.kr/eng/contents/137. [Accessed: 18-May-2026].

[28] Link, M., "Updating of Analytical Models — Basic Procedures and Extensions", in *Modal Analysis and Testing*, J. M. M. Silva and N. M. M. Maia, Eds. Dordrecht: Springer Netherlands, 1999, pp. 281–304.

[29] Link, M., and Hanke, G., "Model Quality Assessment and Model Updating", in *Modal Analysis and Testing*, J. M. M. Silva and N. M. M. Maia, Eds. Dordrecht: Springer Netherlands, 1999, pp. 305–324.

[30] Mottershead, J. E., and Friswell, M. I., "Model Updating In Structural Dynamics: A Survey", *Journal of Sound and Vibration*, vol. 167, no. 2, pp. 347–375, Oct. 1993, https://doi.org/10.1006/jsvi.1993.1340.

[31] Nikodem, F., "Overview of the DLR High Altitude Platform and Scientific Potential of the Technology Demontrator HAP-alpha", presented at the Deutscher Luft- und Raumfahrtkongress 2023, Stuttgart, Deutschland, 2023, https://elib.dlr.de/198509/.

[32] Noll, T., Brown, J., Perez-Davis, M., Ishmael, S., Tiffany, G., and Gaier, M., "Investigation of the Helios Prototype Aircraft Mishap", NASA, Mishap Report, Jan. 2004.

[33] Shariqi, B., and Cesnik, C., "Finite Element Model Updating of a Very Flexible Flying Wing Using Ground Vibration Testing Data", presented at the International Forum on Aeroelasticity and Structural Dynamics, The Hague, The Netherlands, 2024.

[34] Solar Impulse SA, "Solar Impulse - Around the world to promote clean technologies", *Solar Impulse*. [Online]. Available at: http://www.solarimpulse.com/. [Accessed: 24-Mar-2017].

[35] Stéphan, C., Lubrina, P., Sinske, J., Govers, Y., and Lastere, N., "AIRBUS Beluga XL state-of-the-art techniques to perform a Ground Vibration Test campaign of a large aircraft", in *International Forum on Aeroelasticity and Structural Dynamics 2019, IFASD 2019*, Savannah, GA (USA), 2019, https://elib.dlr.de/127959/.

[36] Thiem, C., Buchbach, R., Voß, A., Sinske, J., Soal, K., Tang, M., Volkmar, R., Gundlach, J., and Meier, T., "HAP-alpha: Ground Vibration Test of the Ultra-Lightweight High-Altitude Platform Structure", presented at the International Forum on Aeroelasticity and Structural Dynamics, Göttingen, Germany, 2026.

[37] Voß, A., Buchbach, R., Soal, K., Volkmar, R., Thiem, C., Sinske, J., Gundlach, J., and Niemann, S., "Model Updating Based on Ground Vibration Test and the Influence on Loads and Aeroelasticity for a High Altitude Long Endurance Aircraft", *CEAS Aeronautical Journal*, to be submitted.

[38] Voß, A., Handojo, V., Weiser, C., and Niemann, S., "Preparation of Loads and Aeroelastic Analyses of a High Altitude, Long Endurance, Solar Electric Aircraft", presented at the AEC2020 Aerospace Europe Conference, Bordeaux, France, 2020, https://elib.dlr.de/133496/.

[39] Voß, A., Handojo, V., Weiser, C., and Niemann, S., "Results from Loads and Aeroelastic Analyses of a High Altitude, Long Endurance, Solar Electric Aircraft", *Journal of Aeroelasticity and Structural Dynamics*, vol. 9, no. 1, pp. 1–22, Jan. 2022, https://doi.org/10.3293/asdj.2021.58.

[40] Voß, A., Koch, C., Niemann, S., Mantei, Marius, Handojo, V., and Weiser, C., "Transition From Preliminary to Detailed Design of a Highly Elastic Solar Electric Aircraft", presented at the International Forum on Aeroelasticity and Structural Dynamics, Madrid, Spain, 2022, https://elib.dlr.de/186492/.

[41] Voß, A., Tang, M., and Sinske, J., "Flight Test Instrumentation for Loads and Aeroelastic Analyses of a High Altitude, Long Endurance, Solar Electric Aircraft", presented at the AIAA SciTech, Orlando, Florida, 2026, https://doi.org/10.2514/6.2026-1156.

[42] Weiser, C., and Ossmann, D., "Baseline Flight Control System for High Altitude Long Endurance Aircraft", in *AIAA SciTech 2022 Forum*, San Diego, USA, 2022,

https://arc.aiaa.org/doi/10.2514/6.2022-1390.

[43] Weiser, C., Ossmann, D., and Pfifer, H., “Robust Path-Following Control for High-Altitude Long-Endurance Aircraft”, *Journal of Guidance, Control, and Dynamics*, vol. 7, no. 46, pp. 1416–1424, May 2023, https://arc.aiaa.org/doi/full/10.2514/1.G007326.

[44] Weiser, C., Schulz, S., Voß, A., and Ossmann, D., “Attitude Control for High Altitude Long Endurance Aircraft Considering Structural Load Limits”, presented at the AIAA SCITECH 2023 Forum, National Harbor, Maryland, 2023, https://doi.org/10.2514/6.2023-0106.

[45] “6,000ft Flight Completes Low Altitude Test Campaign”, *Kea Aerospace*, 02-Dec-2024. https://www.keaaerospace.com/news-and-events/6000ft-flight-completes-low-altitude-test-campaign/.

[46] “High-Altitude Platform Systems - Joint Air Power Competence Centre”, 21-Jul-2022. https://www.japcc.org/articles/high-altitude-platform-systems/.

[47] “Media Release: Kea Aerospace Achieves Historic Stratospheric Flight”, *Kea Aerospace*, 11-Feb-2025. https://www.keaaerospace.com/news-and-events/media-release-kea-aerospace-achieves-historic-stratospheric-flight/.

[48] “Meet HAPS: India’s very own UAV that can fly 20 km high and float for months”, *The Indian Express*, 10-Feb-2024. https://indianexpress.com/article/india/meet-haps-indias-very-own-uav-that-can-fly-20-km-high-and-float-for-months-9153929/.

[49] “Swift announces its SULE uncrewed aircraft flies above 55,000 feet”, *Military Aerospace*, 18-Nov-2024. [Online]. Available at: https://www.militaryaerospace.com/uncrewed/article/55243431/swift-announces-sule-uas-tops-55000-feet. [Accessed: 28-Nov-2024].

COPYRIGHT STATEMENT